EVALUATION OF AXIAL LOAD-BEARING CAPACITY OF CONCRETE COLUMNS STRENGTHENED BY A NEW SECTION ENLARGEMENT METHOD

Meijing HAO[1], Wenzhong ZHENG[1,2,3*], Wei CHANG[1]

[1]School of Civil Engineering, Harbin Institute of Technology, 150090 Harbin, China
[2]Key Lab of Structures Dynamic Behavior and Control Ministry of Education,
Harbin Institute of Technology, 150090 Harbin, China
[3]Key Lab of Smart Prevention and Mitigation of Civil Engineering Disasters of the Ministry
of Industry and Information Technology, Harbin Institute of Technology, 150090 Harbin, China

Abstract. The objective of this study is to evaluate the axial load-bearing capacity of section-enlargement concrete columns. To reach the objection, a new strengthened method in which columns are jacketed with a large welded octagonal stirrup at the center and four spiral stirrups at the corners of column is developed. The new section-enlargement method avoids interrupting existing columns and improves the reliability of strengthened part, besides, the confining stress generated by octagonal stirrup and spiral stirrups enhances the compressive strength and deformability of strengthened columns. In addition, sixteen large-scale concrete columns strengthened by the new strengthened method were tested under axial compressive loads. The experimental results show that the axial compression ratio of existing column generates stress-strain lag in strengthened part and decreases the load-bearing capacity of specimens; the stirrups in strengthened part significantly enhance the axial load-bearing capacity of specimens. According to confinement conditions, the cross-section of specimens is divided into five parts and the confinement factor for each part is calculated to establish the prediction models for the load-bearing capacity of specimens. Furthermore, by comparing the results between the developed model and existing models, the developed model has high accuracy in evaluating the load-bearing capacity of strengthened columns.

Keywords: strengthened concrete columns, section-enlargement method, axial load-bearing capacity, confined concrete, prediction models.

Introduction

In reinforced concrete structures, the section-enlargement method is an efficient method to improve the axial load-bearing capacity of concrete components (Adilson et al., 2008; Cao et al., 2017; Hwang et al., 2020; Thermou et al., 2014; Zhang, 2004). In Figure 1 (Ministry of Housing and Urban-rural Development of the People's Republic of China, 2014), the traditional section-enlargement method needs to drill holes into the existing column and then embed the U-shaped stirrups which may cause damage to the existing column. However, due to the load on the existing column before strengthened, the existing column may be broken firstly when the strengthened concrete column is loaded. Subsequently, the U-shaped stirrups embedded into the existing column become weak and the confinement effect of the U-shaped stirrups becomes in-

significant. Thus, it is necessary to improve the traditional section enlargement method to ensure the strengthened concrete column can be performed well.

Compared with other strengthening methods, the section-enlargement method is simple for construction and have good economic benefit owing to the full use of the existing components. Moreover, the method can significantly enhance the load-bearing capacity, the stiffness of the components and the stability of the structures. In this study, a new section-enlargement method adopting the multi-spiral stirrups for concrete columns is developed. In Figure 2, an octagonal stirrup consisting of two identical parts joined by welding is applied at the center of the cross-section. The new section-enlargement method avoids drilling holes and embedding stirrups into the

*Corresponding author. E-mail: *wzz13136691863@163.com*

Figure 1. Application of the traditional section-enlargement method to a column

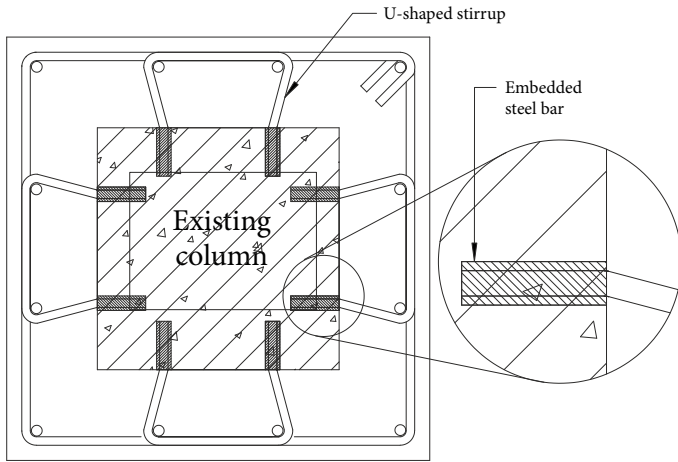

Figure 2. Application of the proposed section-enlargement method to a column

existing column and the reliability of the strengthened part was relatively improved. The confining stress generated by the octagonal stirrup can successfully increase the confinement for the existing column and most part of the strengthened concrete. Further, four spiral stirrups enhance the lateral confinements at the four corners of the enlarged column. The production of large octagonal stirrup and spiral stirrups in the factory is automatic and efficient and the construction process is cost-effective and time-saving.

Based on a series of experimental results, Ersoy et al. (1993) indicated that the load-bearing capacity decreased by about 10% when the calculation models considered the two-stage loading process on the existing part of the column. Thus, the strength reduction coefficient was introduced to evaluate the effects of the axial compression ratio of existing columns when evaluated the load-bearing capacity of strengthened column (Ministry of Housing and Urban-rural Development of the People's Republic of China, 2014; Zhang et al., 2001; Tang, 2000). Su et al. (1997) introduced an enhancement coefficient into the existing equations to calculate the confinement effect of the strengthened part. In order to considered the confinement of stirrups, Liu (2005) adopted the prediction models proposed by Mander and Priestley (1988) for evaluating the confinements of stirrups. However, the researches on evaluating the load-bearing capacity of strengthened columns were limited by considering both the axial compression ratio of existing columns and the confinement effect of stirrups.

In this study, sixteen large-scale concrete columns have been strengthened by a large octagonal stirrup at the center and four spiral stirrups at the corners of the cross-section. All specimens have been tested under axial compressive load to evaluate the load-bearing capacity of the section-enlarged concrete columns. The effects of the axial compression ratio of existing columns and the lateral confinement of stirrups in strengthened part on the load-bearing capacity of specimens have been analyzed.
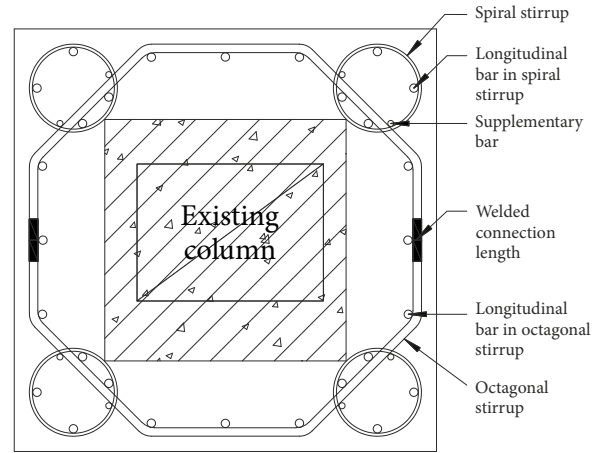
Moreover, an analytical model for evaluating the load-bearing capacity of strengthened concrete columns has been developed.

1. Experimental programs

1.1. Specimens' design

Sixteen large-scale concrete columns strengthened by the section-enlargement method developed in this study were prepared and tested under axial compressive load. All specimens consisted of the existing part and the strengthened part. Based on the previous studies (Julio & Branco, 2008; Vandoros & Dritsos, 2008), if the interfaces were well roughened, the axial load-bearing capacity of specimens minimally affected by the old-new concrete interface. Thus, the interface of old concrete was supposed well roughening before strengthened. The existing columns were 400×400 mm^2 in cross-section and 2100 mm in height, while the specimens were 700×700 mm^2 in cross-section and 2100 mm in height after strengthened. The overlapped area between spiral stirrups and octagonal stirrup was 24.32% of the area of a spiral stirrup. Figure 3 shows the reinforcement arrangements in specimens. Table 1 listed the design details of all specimens. The axial compression ratios of existing columns were 0, 0.1, 0.2 and 0.3, corresponding to the loads of existing columns were 0, 489.12 kN, 978.24 kN and 1467.36 kN, respectively. The volumetric ratios of octagonal stirrup were 2.1%, 1.7%, 1.2% and 0.9%, and the volumetric ratio of four small spiral stirrups were 2.3%, 1.3%, 0.9% and 0.7%.

In existing columns, Grade 400 reinforcing bars in the diameter of 10 mm were used as rectilinear hoops spaced at 100 mm; and eight Grade 400 reinforcing bars in the diameter of 18 mm were applied as longitudinal bars located at the corners and the middle of the side length of the rectilinear hoops. The volumetric ratio of rectilinear hoops and the ratio of longitudinal reinforcement were 1.03% and 1.27%, respectively. The concrete strength of existing columns was Grade 30. The compression load of exist-

a) Existing column

b) Specimens with $\rho_{sv1} = 2.1\%$

c) Specimens with $\rho_{sv1} = 1.7\%$

d) Specimens with $\rho_{sv1} = 1.2\%$
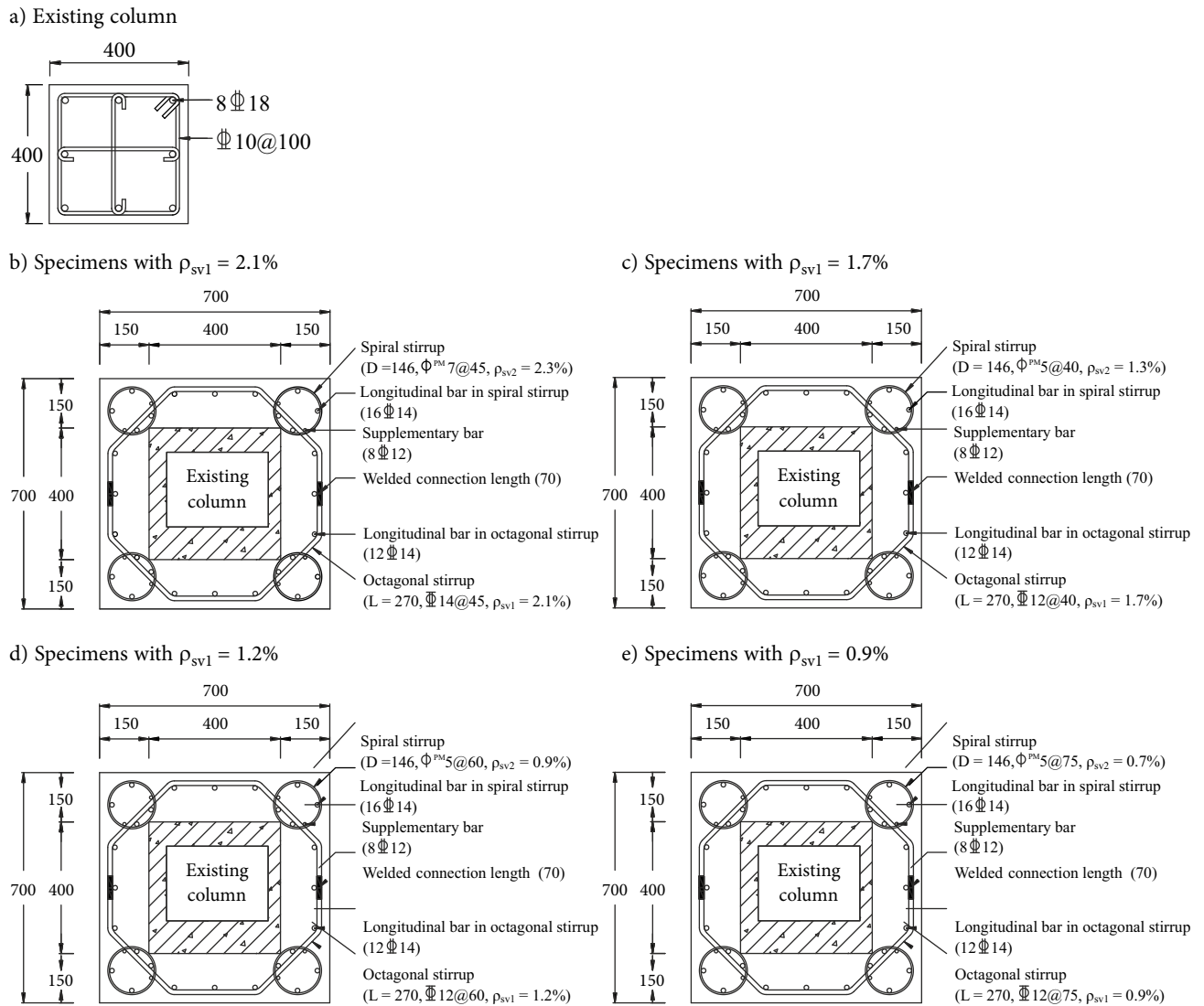

e) Specimens with $\rho_{sv1} = 0.9\%$

Figure 3. Reinforcement arrangements in existing column and specimens (Unit: mm)

ing column was applied through two or four prestressed reinforcing bars of Grade 1080 shown in Table 1. An expanding parts with 1000×1000 mm² in cross-section and 300 mm in height were constructed at both ends of existing column to let axial load applied on the existing column. Figure 4 shows the design details of expanding part. In the upper expanding part, four holes in a diameter of 150 mm were formed by the PVC pipes corresponding to the positions of the four spiral stirrups which concrete can be poured into the strengthening part of specimens. Due to the local pressure generated by the prestressed reinforcing bars, reinforcing mesh was used in the corresponding parts. The prestressed reinforcing bars were symmetrically arranged based on the axial compression ratio of existing column. Figure 5 shows the test setup for prestressing the reinforcing bars. Each prestressed reinforcing bar had two strain gauges in the middle and one pressure transducer at the top. The hydraulic jack applied an axial load at a low level to a distributing girder, and then, the position of the distributing girder was adjusted so that the loads on each prestressed reinforcing bar were equal. After tightening the nuts on the prestressed reinforcing bars, the hydraulic jack was removed. Then, the load showed by the two strain gauges was observed until the load was stable. If the average load of the two strain gauges was smaller than the designed load, the prestressing was repeated with additional tension. In order to prevent the loss of prestress in the reinforcing bars, the symmetrical prestressed reinforcing bars had an exceed tension.

In strengthened part, sixteen Grade 400 reinforcing bars in the diameter of 14 mm were used as longitudinal bars in four spiral stirrups and octagonal stirrups. The longitudinal reinforcement ratio in strengthened part was 1.30%. Grade 800 spiral stirrups in the diameters of 5mm and 7 mm and half of the Grade 500 octagonal stirrups in the diameters of 12 mm and 14 mm were carried out in factory. The concrete strength of strengthened part was Grade 40.

Table 1. Specimens details

| Specimens | Stirrups in strengthened part | | | | | Axial compression ratio of existing columns | | | |
| | d_1, mm | d_2, mm | S, mm | ρ_{sv1}, % | ρ_{sv2}, % | β | P_{exi}, kN | Prestressed reinforcing bar | |
								n	d_3, mm
ACS-1	14	7	45	2.1	2.3	0.3	1467.36	4	32
ACS-2	12	5	40	1.7	1.3	0.3	1467.36	4	32
ACS-3	12	5	60	1.2	0.9	0.3	1467.36	4	32
ACS-4	12	5	75	0.9	0.7	0.3	1467.36	4	32
ACS-5	14	7	45	2.1	2.3	0.2	978.24	2	25
ACS-6	12	5	40	1.7	1.3	0.2	978.24	2	25
ACS-7	12	5	60	1.2	0.9	0.2	978.24	2	25
ACS-8	12	5	75	0.9	0.7	0.2	978.24	2	25
ACS-9	14	7	45	2.1	2.3	0.1	489.12	2	25
ACS-10	12	5	40	1.7	1.3	0.1	489.12	2	25
ACS-11	12	5	60	1.2	0.9	0.1	489.12	2	25
ACS-12	12	5	75	0.9	0.7	0.1	489.12	2	25
ACS-13	14	7	45	2.1	2.3	0	0		–
ACS-14	12	5	40	1.7	1.3	0	0		–
ACS-15	12	5	60	1.2	0.9	0	0		–
ACS-16	12	5	75	0.9	0.7	0	0		–

Note: ACS is the abbreviation of Axial Compression Specimens; $\alpha_c = \dfrac{\sigma_{c2}}{f_c} = 2\sqrt{1-\beta} + \beta - 1$ and d_2 are the diameters of the octagonal stirrups and the spiral stirrups in strengthened part of specimens, respectively; S is the spacing of stirrups; $N = \varphi\left(f_{c0}A_{c0} + f_{y0}'A_{s0}' + \alpha_{cs}\left(f_{c0}A_{c0} + f_y'A_s' \right) \right)$ and $\alpha_{cs} = 0.8$ are the volumetric ratios of the octagonal stirrups and the spiral stirrups in strengthened part, respectively; and β is the axial compression ratio of existing columns. P_{exi} is the axial load in existing column before strengthening; n is the number of the prestressed reinforcing bars; d_3 is the diameter of prestressed reinforcing bars.
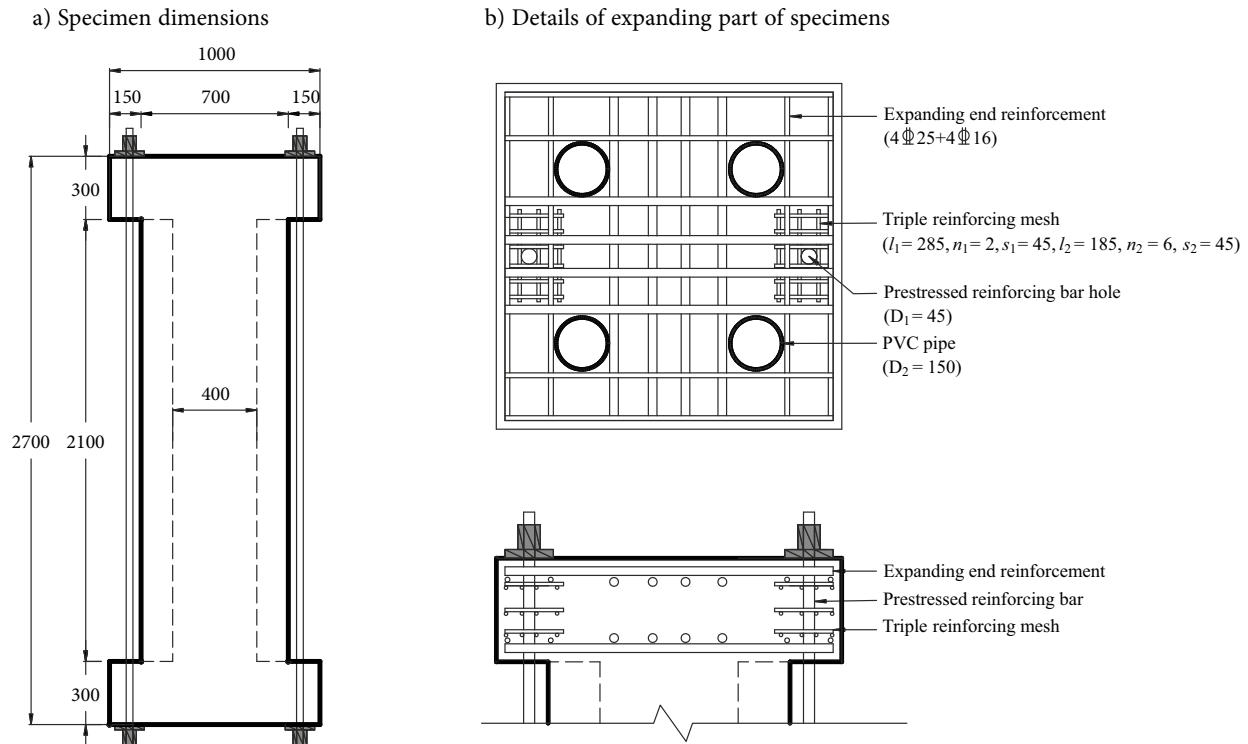
a) Specimen dimensions

b) Details of expanding part of specimens

Figure 4. Design details of expanding part (Unit: mm)

a) Schematic diagram of test setup   b) Physical diagram of test setup
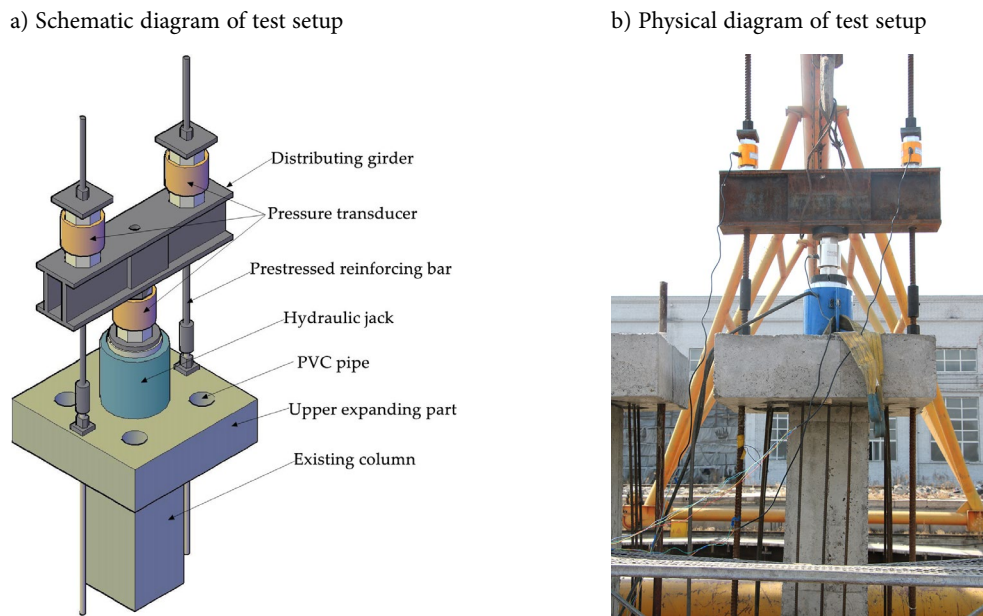

Figure 5. Test setup for prestressing reinforcing bars

The construction procedure of specimens is described as follows: (1) the two expanding part and existing column were constructed and the four holes with the diameter of 150 mm were formed in the top expanding part, corresponding to the positions of four spiral stirrups; (2) the load on existing column was applied by tensioning prestressed reinforcing bars; (3) the longitudinal bars in octagonal stirrups were arranged according to the design requirements; (4) the octagonal stirrups were welded together with connection length of $5d_1$; (5) the spiral stirrups were pushed to the corresponding positions from the horizontal direction; (6) the longitudinal bars in the four spiral stirrups were inserted from the four holes in the top expanding part and bounded with spiral stirrups; (7) the concrete of strengthened part was poured from the four holes in the top expanding part, and specimens were completed.

1.2. Material properties

To determine the compressive strength of concrete used in all specimens, according to the requirements of GB 50010-2010 (Ministry of Housing and Urban-rural Development of the people's Republic of China, 2010) three 150×150×150 mm concrete cubes were prepared. The com-

pressive strength of C30 and C40 cubes were 40.23 MPa and 51.49 MPa, respectively. The axial compressive strength of C30 and C40 were 30.57 MPa and 39.51 MPa, respectively. Furthermore, three samples of each type reinforcing bars used in specimens were tested under axial tension. The mechanical properties and the stress-strain curves of reinforcing bars are shown in Table 2 and Figure 6, respectively.
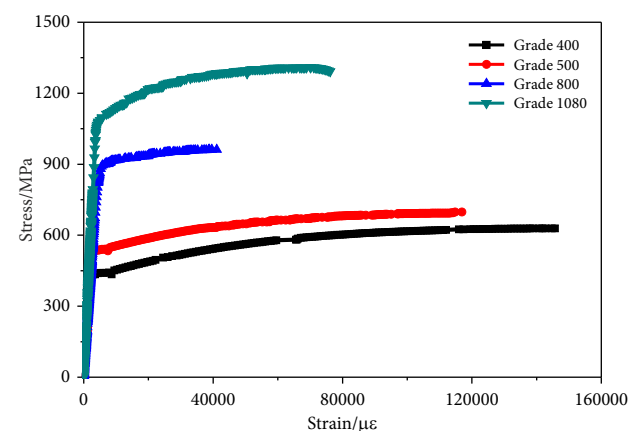

Figure 6. Stress-strain curves of reinforcing bars

Table 2. Mechanical properties of reinforcing bars

Type of steel	Proportional limit, MPa	Yield stress, MPa	Ultimate stress, MPa	Ultimate strain, %	Elastic modulus, MPa	Yield plateau, %
Grade 400	436.7	436.7	629.0	14.5	200000	0.577
Grade 500	536.1	536.1	698.6	11.7	200000	0.475
Grade 800	672.9	899.6	962.0	4.1	205000	–
Grade 1080	999.5	1097	1310.1	7.0	200000	–

1.3. Test setups

Figure 7 shows the loading equipment and the test setup of specimens. The loading equipment is a hydraulic testing machine with a capacity of 30,000 kN at Harbin Institute of Technology. To ensure the axial load distributed uniformly, both ends of specimen were polished smoothly and some sand was put on the top of specimens. Furthermore, both ends of the specimen column were mounted by customised steel clamps to ensure the ends of specimens were not damaged.

To ensure test apparatuses work well, a preloading was conducted. The load-displacement controlled scheme was applied to specimens in accordance with GB/T 50152-2012 (Ministry of Housing and Urban-rural Development of the People's Republic of China, 2012). The loading scheme was divided into four steps: (1) the scheme was controlled by applying the load at a rate of 4 kN/s in a monotonic manner until cracks appeared on the surface of the column; (2) the scheme was controlled by the displacement at a rate of 0.5 mm/min until the load capacity of the column over peak stress; (3) the scheme was controlled by the displacement at a rate of 1.0 mm/min until the load capacity of the column reached 50% of the peak stress; and (4) the scheme was controlled by the displacement at a rate of 2.0 mm/min until the specimens were damaged.

Strain gauges were placed on the longitudinal reinforcements, stirrups and concrete cover to measure the vertical and horizontal deformations of steel reinforcements and concrete, respectively. Figure 8 shows the distribution of strain gauges. The strain gauges were placed at the middle of specimens with a range of 700 mm. The distribution of total 46 strain gauges on each existing column was listed as follows: four steel strain gauges were placed at two longitudinal reinforcements located at the corners and the middle of the side length of the rectilinear hoops to measure the vertical deformation of longitudinal reinforcements, and 14 steel strain gauges were placed uniformly at three rings of the stirrups at the middle of specimens to measure the horizontal deformation of the existing columns. The distribution of total 122 steel strain gauges on the strengthening part of each specimen was listed as follows: four steel strain gauges were placed at two longitudinal reinforcements located at each spiral stirrups, and four steel strain gauges were placed at two longitudinal reinforcements located at octagonal stirrups to measure the vertical deformation of strengthening part; 66 steel strain gauges were placed at three rings of octagonal stirrups in the middle of specimens to measure the horizontal deformation of octagonal stirrups; and 12 steel strain gauges were placed at the three circles of each spiral
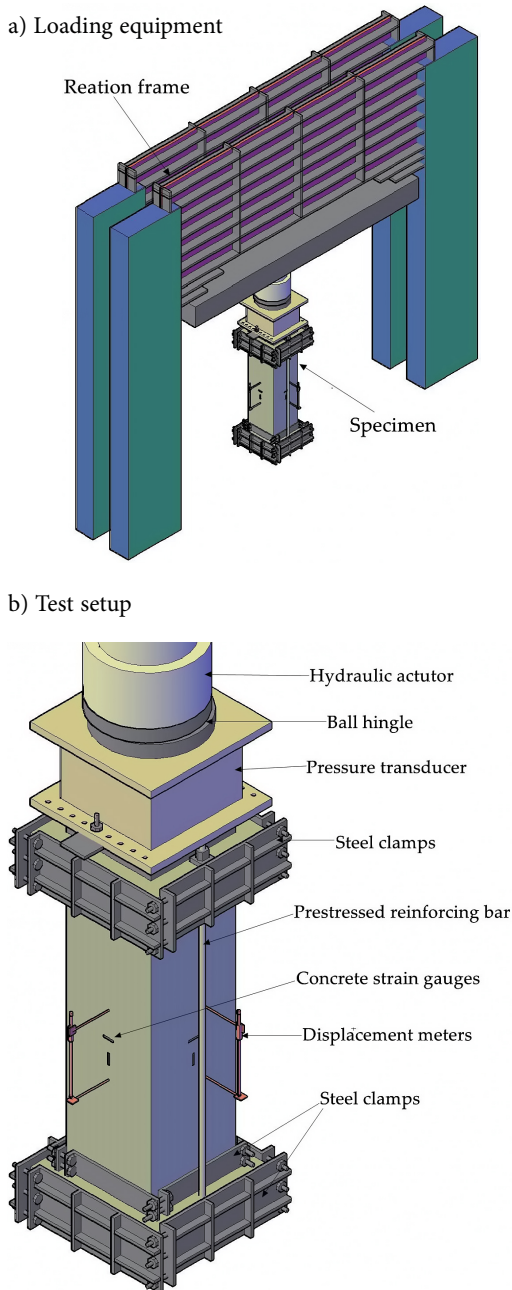

a) Loading equipment

b) Test setup

Figure 7. Loading equipment and test setup

700

1-1

Concrete strain gauge
Octagonal stirrup strain gauge
Spiral stirrup strain gauge
Existing column stirrup strain gauge
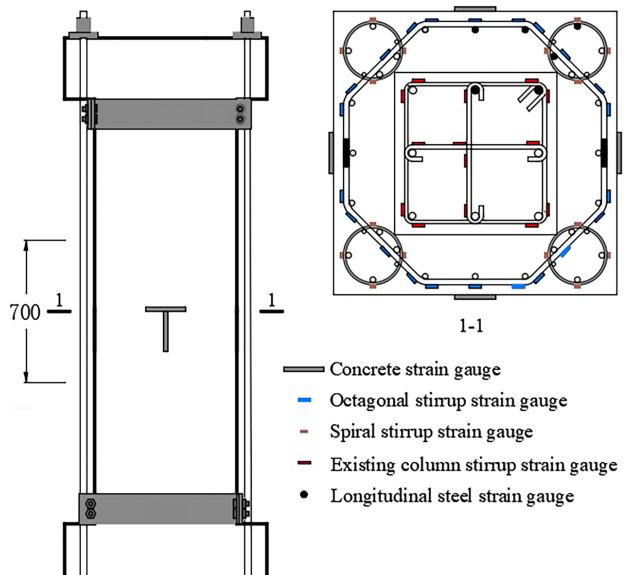Longitudinal steel strain gauge

Figure 8. Distribution of strain gauges (Unit: mm)

stirrup in the middle of specimens to measure the horizontal deformation of spiral stirrups. Further, to measure the vertical and horizontal deformations of concrete cover, four vertical and four horizontal concrete strain gauges were placed on the surface of specimens, respectively. Two steel strain gauges were placed on each prestressed reinforcing bar to monitor the load applied on prestressed reinforcing bars. In addition, four displacement meters were installed in the middle of specimens with 350 mm gauge length to measure the vertical deformation of specimens. A high-speed data acquisition was utilized to collect experimental data from strain gauges and displacement meters.

2. Test results and discussion

2.1. Failure patterns

The failure patterns of sixteen specimens were complex due to the multiple confinement generated by numerous stirrups in strengthened parts. The typical failure patterns of specimens were shown in Figure 9. Specimens failed through the buckling of longitudinal bars, followed by the concrete crushed and stirrup fractured. The failure process of specimens can be divided into four stages during the loading scheme. The first stage was from the beginning of loading scheme to the beginning of the appearance of minor vertical cracks on the surface of specimens. The second stage started from the beginning of the minor vertical cracks appeared until specimens reached the peak axial load. In this stage, the cracks began to be widened and lengthen and specimens reached peak load after the slight spalling of concrete cover. In addition, the forces on prestressed reinforcing bars were almost unloaded and longitudinal reinforcement yielded. The third stage started from the peak load to the fracture of spiral stirrups. In this stage, the vertical cracks transformed into severe cracks and core concrete exterior. Then, the concrete confined by spiral stirrups at the corner crushed and spiral stirrups fractured because of the larger dilation of concrete and lower volumetric ratio compared with octagonal stirrups. The fourth phase started the fracture of spiral stirrups to the load-bearing capacity decreased suddenly, caused by the fracture of octagonal stirrups. In this stage, the octagonal stirrups were tensioned due to the dilation of concrete. The load-bearing capacity decreased significantly when the first octagonal stirrup fractured. Subsequently, more octagonal stirrups fractured owing to the sudden load transfer caused by the fracture of the first octagonal stirrup.
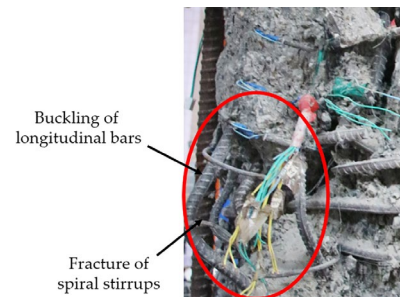
2.2. Effect of axial compression ratio of existing columns on load-bearing capacity of specimens

Figure 10 shows the effect of the axial compression ratio of existing columns on the axial load-bearing capacity of specimens. P_{test} is the axial load-bearing capacity of specimens acquired by eliminating the residual value of

a) Failure patterns of strengthened RC columns

b) Local details of spiral stirrups

Buckling of
longitudinal bars

Fracture of
spiral stirrups

c) Local details of octagonal stirrups

Buckling of
longitudinal bars

Fracture of
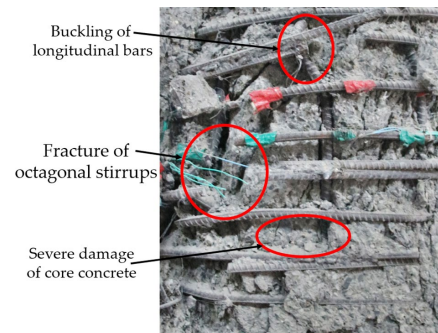octagonal stirrups

Severe damage
of core concrete

Figure 9. Typical failure patterns of strengthened RC columns

prestressed reinforcing bars. P_0 is the axial load-bearing capacity of specimens in which the axial compression ratio of existing column is zero. The strength ratio (P_{test}/P_0) of specimens has been used to evaluate the effect of the axial compression ratio of existing columns. The result shows that the axial load-bearing capacity of specimens decreases with increasing the axial compression ratio of existing columns. In particular, as the axial compression ratio increases by 0.1, the axial load-carrying capacity of specimens decreases by 2.5% in the maximum.
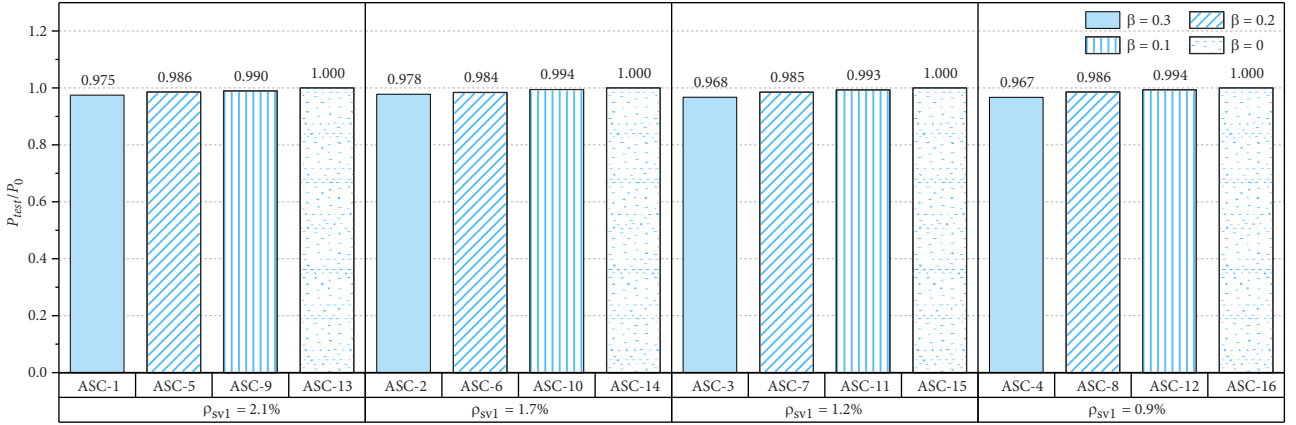
Figure 10. Effect of axial compression ratio of existing columns on the load-bearing capacity of specimens

The existing columns were loaded before strengthened and the strengthened part carried the load together with the existing columns when the new load was applied. When existing column reached the peak load, it was with high probability that the strengthened part could not reach the peak load. Thus, the stress and strain in the strengthened part lagged behind existing columns. The enhancement effect of strengthened part decreased if the concrete of existing columns was in a high stress level before strengthening. Thus, the compressive strength of strengthened part needed to be reduced based on the axial compression ratio of existing column. Accordingly, the previous studies developed the reduction factors for evaluating the axial load-bearing capacity of strengthened part (Tang, 2000; Su et al., 1997; Luo, 1989; Cheng, 2003; Liao, 2006). α_c and α_s are the reduction factors of concrete and longitudinal bars generally used for evaluating the load-bearing capacity of the strengthened part of strengthened columns, respectively, which are listed as follows:

$$\alpha_c = \frac{\sigma_{c2}}{f_c} = 2\sqrt{1-\beta} + \beta - 1; \tag{1}$$

$$\alpha_s = \frac{\sigma_{s2}}{f_y'} = \frac{E_{s2}}{500 f_y'}\sqrt{1-\beta}, \tag{2}$$

where, σ_{c2} and σ_{s2} are the stress of concrete and longitudinal bars in strengthened part when existing column reached the limited state, respectively; f_c is the compressive strength of concrete in strengthened par; f_y' and E_{s2} are the yield strength and elasticity modulus of longitudinal reinforcements in strengthened part, respectively.

2.3. Effect of volumetric ratio of stirrups in strengthened part on load-bearing capacity of specimens

In order to evaluate the confinement effect of stirrups in the strengthened part of specimens, an analytical load of section-enlargement column $P_{analysis}$ is defined as follows:

$$P_{analysis} = f_{c0}A_{c0} + f_{y0}'A_{s0}' + \alpha_c f_c A_c + \alpha_s f_y'A_s', \tag{3}$$

where f_{c0} is the compressive strength of concrete in ex-

isting column; A_{c0} is the cross-section area of concrete in existing column; f_{y0}' is the yield strength of the longitudinal reinforcements in existing column; A_{so}' is the cross-section area of the longitudinal reinforcements in existing column; A_c is the cross-section area of concrete of strengthened part; and A_s' is the cross-section area of the longitudinal reinforcements in strengthened part. $P_{analysis}$ has been calculated by the measured material strengths listed in Table 2.

The analytical load-bearing capacity $P_{analysis}$ represents the axial compressive strength of section-enlargement columns neglecting the confinement effect of stirrups in strengthened part. In Table 3, the load-bearing capacity ratio of specimens is defined as $P_{test}/P_{analysis}$, which is an indicator of the axial load-bearing capacity enhancement of specimens from the confinement of stirrups in strengthened part. The load-bearing capacity ratio of specimens with the same axial compression ratio of existing columns increases following the volumetric ratio of stirrups from 0.9% to 2.1%, especially, the load-bearing capacity ratio of specimens ranges from 1.26 to 1.28 when the volumetric ratio of stirrups is 2.1% in the maximum. The compressive strength of concrete was enhanced by octagonal stirrups and four spiral stirrups because stirrups generate higher lateral confining stress and a larger volumetric ratio of stirrups resulting in a larger load-bearing capacity ratio of specimens.

Figure 11 shows the normalized load-displacement curves of specimens. The axial loads have been normalized to the analytical load of the section-enlargement columns for comparison purpose. In Figure 10, when the axial compression ratio of existing column remains at a certain value, the axial load-bearing capacity of specimens increases with the increase of the volumetric ratio of stirrups from 0.9% to 2.1%. The large volumetric ratio of stirrups effectively enhances the axial load-carrying capacity of specimens.

The average concrete compressive strength $f_{c,average}$ is derived as follows:

$$f_{c,average} = \frac{f_{c0}A_{co} + f_c A_c}{A_{co} + A_c}. \tag{4}$$

Table 3. Confinement effect of stirrups in strengthened part of specimens

| Specimens	P_{test}, kN	$P_{analysis}$, kN	$f_{c,average}$, MPa	$f_{cc,average}$, MPa	$\dfrac{P_{test}}{P_{analysis}}$	$\dfrac{f_{cc,average}}{f_{c,average}}$
ACS-1	25380	19790	35.63	48.47	1.28	1.36
ACS-2	24810	19790	35.63	47.12	1.25	1.32
ACS-3	23807	19790	35.63	44.75	1.20	1.26
ACS-4	23000	19790	35.63	42.84	1.16	1.20
ACS-5	25680	20090	36.04	48.14	1.28	1.34
ACS-6	24968	20090	36.04	46.30	1.24	1.28
ACS-7	24225	20090	36.04	44.47	1.20	1.23
ACS-8	23445	20090	36.04	42.59	1.17	1.18
ACS-9	25768	20293	36.27	48.78	1.27	1.35
ACS-10	25224	20293	36.27	47.49	1.24	1.31
ACS-11	24440	20293	36.27	45.64	1.20	1.26
ACS-12	23631	20293	36.27	43.72	1.16	1.21
ACS-13	26038	20574	36.33	48.82	1.27	1.34
ACS-14	25371	20574	36.33	47.24	1.23	1.30
ACS-15	24606	20574	36.33	45.43	1.20	1.25
ACS-16	23783	20574	36.33	43.48	1.16	1.20
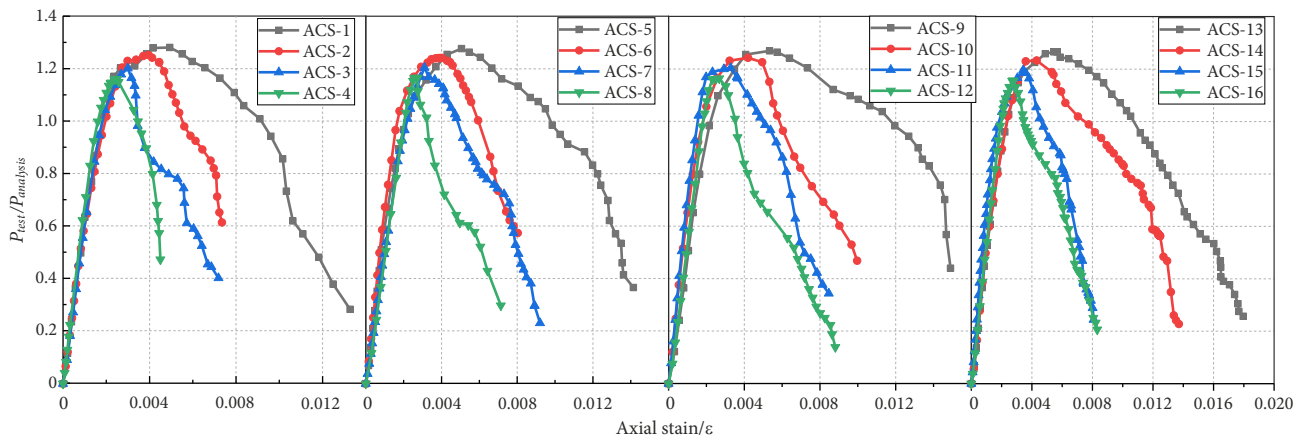
Figure 11. Normalized load-displacement curves of specimens

Correspondingly, the average compressive strength $f_{cc,average}$ of confined concrete has been used to evaluate the confinement effect of the lateral reinforcement in strengthened part. Assuming that the concrete in existing part is crushed and the longitudinal bars are yielded at the peak load, the compressive strength $f_{cc,average}$ of confined concrete can be determined as follows:

$$f_{cc,average} = \frac{P_{test} - \alpha_c f_c A_{c,cover} - f_{y0}{}' A_{s0}{}' - \alpha_s f_y{}' A_s{}'}{A_{co} + A_c - A_{c,cover}}, \quad (5)$$

where $A_{c,cover}$ is the cross-section area of concrete cover of strengthened part.

A compressive strength ratio of concrete evaluating the confinement effect of stirrups in strengthened part is defined as $f_{cc,average}/f_{c,average}$. As shown in Figure 12, the compressive strength ratios of concrete are in the range of 1.18–1.21, 1.23–1.26, 1.28–1.32 and 1.34–1.36, corre-

sponding to the specimens with the volumetric ratio of stirrups are 0.9%, 1.2%, 1.7% and 2.1%, respectively. The highly confined concrete surrounded by octagonal stirrups and spiral stirrups had high compressive strength of concrete.

3. Evaluation of axial load-bearing capacity

3.1. Analytical modeling

The axial load-bearing capacity of the section-enlargement column is contributed from each structural material. In order to calculate the axial load-bearing capacity of specimens, the constitutive model of materials is specified as follows. Considering the confinement effect contributed from the octagonal stirrups, spiral stirrups and concrete of strengthened part of specimens, as shown in Figure 13, the concrete in the cross-section of specimens is categorized
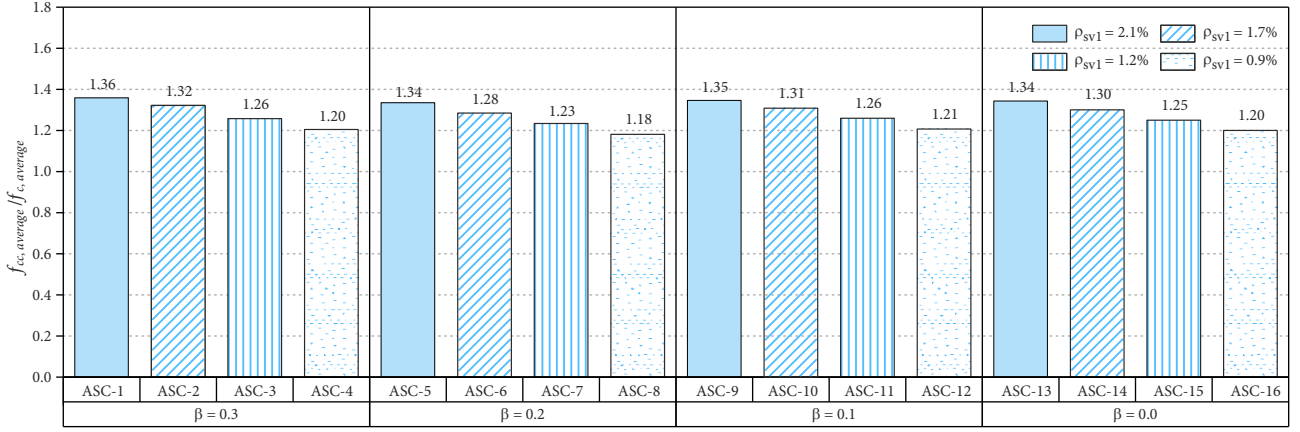
Figure 12. Effect of volumetric ratio of stirrups on load-bearing capacity of specimens
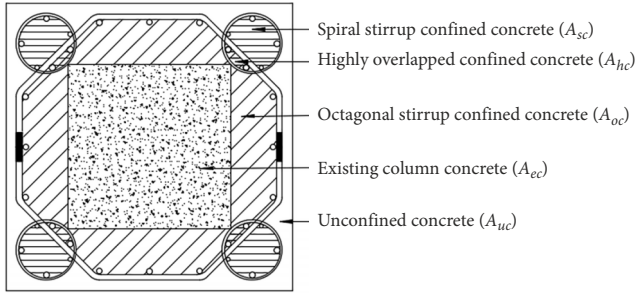

Figure 13. Five confinement area in specimens

into five parts: concrete in existing column, concrete confined by octagonal stirrups, concrete confined by spiral stirrups, highly overlapping concrete confined by both octagonal stirrups and spiral stirrup, and unconfined concrete.

In this study, the stress-strain relationships of confined concrete proposed by Mander and Priestley (1988) have been used for evaluating the confinement effects of stirrups in strengthened part. The load-bearing capacity of specimens can be calculated based on the compressive strength f_{cc}' and peak strain ε_{cc} of confined concrete, respectively. The f_{cc}' and ε_{cc} can be calculated as follows:

$$\varepsilon_{cc} = \varepsilon_{c0}\left[1+5\left(\frac{f_{cc}'}{f_{co}'}-1\right)\right];\tag{6}$$

$$f_{cc}' = kf_{co}';\tag{7}$$

$$k = -1.254 + 2.254\sqrt{1+\frac{7.94f_l'}{f_{co}'}} - 2\frac{f_l'}{f_{co}'};\tag{8}$$

$$f_l' = f_l k_e;\tag{9}$$

$$k_e = \frac{1-\dfrac{s'}{2d_s}}{1-\rho_{cc}},\tag{10}$$

where f_{co}' and ε_{co} are the compressive strength and peak strain of unconfined concrete, respectively; k is the confinement factor of confined concrete; f_l' is the effective lateral confining stress; f_l is the lateral confining stress; k_e is the confinement effectiveness coefficient; s' is the clear

spacing of spiral stirrups or hoops; d_s is the diameter of spiral stirrups; and ρ_{cc} is the longitudinal reinforcement ratio.

Figure 14 shows the stress analysis of the stirrups in the strengthened part of specimens. The stress in octagonal stirrup can be derived based on the equilibrium of forces as follows:

$$f_{lo1} = \frac{\sqrt{2}f_{st1}A_{st1}}{b_{cor}s};\tag{11}$$

$$f_{lo2} = \frac{2f_{st1}A_{st1}}{b_{cor}s}.\tag{12}$$

The weighted arithmetic mean of the octagonal stirrup can be described as follows:

$$f_{lo} = \frac{\sqrt{2}}{1+\sqrt{2}}f_{lo1} + \frac{1}{1+\sqrt{2}}f_{lo1} = \frac{4f_{st1}A_{st1}}{(1+\sqrt{2})b_{cor}s} = \frac{1}{1+\sqrt{2}}\rho_{sv1}f_{st1},\tag{13}$$

where

$$\rho_{sv1} = \frac{\dfrac{8b_{cor}}{1+\sqrt{2}}A_{st1}}{2(1+\sqrt{2})(\dfrac{b_{cor}}{1+\sqrt{2}})^2 s} = \frac{4A_{st1}}{b_{cor}s}.\tag{14}$$

Moreover, the stress in spiral stirrup can be derived based on the equilibrium of forces as follows:

$$f_{ls} = \frac{2f_{st2}A_{st2}}{D_{cor}s} = \frac{1}{2}\rho_{sv2}f_{st2},\tag{15}$$

where

$$\rho_{sv2} = \frac{\pi D_{cor}A_{st2}}{\dfrac{1}{4}D_{cor}^2 s} = \frac{4A_{st2}}{D_{cor}s},\tag{16}$$

where f_{lo} and f_{ls} are the lateral confining stress of octagonal stirrup and spiral stirrup, respectively; f_{st1} and A_{st1} are the tensile stress and the cross-sectional area of octagonal stirrup, respectively; f_{st2} and A_{st2} are the tensile stress and the cross-section area of spiral stirrup, respectively; b_{cor} is length of the core concrete confined by octagonal stirrup; D_{cor} is the diameter of core concrete confined by spiral stirrup.

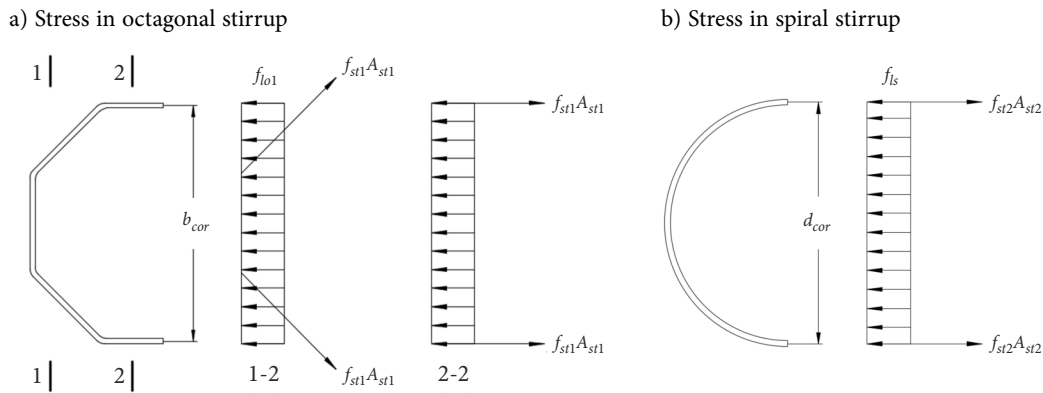a) Stress in octagonal stirrup   b) Stress in spiral stirrup

Figure 14. Analysis of stress in stirrups

3.2. Evaluation of axial load-bearing capacity

The confinement factors for each part in section-enlarged column can be described as follows: k_{ec} is the confinement factor of existing column, k_{oc} is the confinement factor of the concrete confined by octagonal stirrups, k_{sc} is the confinement factor of the concrete confined by spiral stirrups, k_{hc} is the confinement factor of the overlapped concrete confined by both octagonal stirrups and spiral stirrups which was the minimum value between the k_{oc} and k_{sc}. The confinement factors of specimens are shown in Table 4.

The calculation models of the axial load-bearing capacity of specimens were based on the assumptions as follows: (1) the axial strains are compatible in each part of specimens; (2) the strengthened column reaches the limited states of the load-bearing capacity when the compressive strain of the concrete in existing column is ε_{co} and the longitudinal bars in existing column reach the yield

strength. The axial load-bearing capacity of specimens can be calculated through assumption of the individual strength from each part, as follows:

$$P_u = f_{ec} A_{ec} + f_{y0}{}' A_{s0}{}' + \alpha_c \left[f_{oc} A_{oc} + f_{sc} A_{sc} + f_{hc} A_{hc} + f_{uc} A_{uc} \right] + \alpha_s f_y{}' A_s{}', \quad (17)$$

where f_{ec} and A_{ec} are the compressive strength and the cross-section area of concrete in existing column, respectively; f_{oc} and A_{oc} are the compressive strength and the cross-section area of the concrete confined by octagonal stirrups, respectively; f_{sc} and A_{sc} are the compressive strength and the cross-section area of the concrete confined by spiral stirrups, respectively; f_{hc} and A_{hc} are the compressive strength and the cross-section area of the overlapped concrete confined by both the octagonal and spiral stirrups, respectively; f_{uc} and A_{uc} are the compressive strength and the cross-section area of unconfined concrete. The calculated results are shown in Table 4.

Table 4. Confinement factors and axial load-bearing capacity of specimens

Specimens	k_{ec}	k_{oc}	k_{sc}	k_{hc}	P_u	P_{test}	Error
ACS-1	1.42	1.34	1.44	1.34	25203	25380	−0.69%
ACS-2	1.30	1.24	1.25	1.24	23522	24810	−5.19%
ACS-3	1.17	1.14	1.17	1.14	21969	23807	−7.72%
ACS-4	1.12	1.09	1.08	1.08	21170	23000	−7.96%
ACS-5	1.45	1.36	1.31	1.31	25548	25680	−0.51%
ACS-6	1.32	1.26	1.23	1.23	24027	24968	−3.77%
ACS-7	1.27	1.21	1.19	1.19	23365	24225	−3.55%
ACS-8	1.21	1.17	1.12	1.12	22549	23445	−3.82%
ACS-9	1.48	1.39	1.55	1.39	26706	25768	3.64%
ACS-10	1.39	1.31	1.26	1.26	25041	25224	−0.73%
ACS-11	1.26	1.20	1.16	1.16	23370	24440	−4.38%
ACS-12	1.14	1.11	1.07	1.07	21916	23631	−7.26%
ACS-13	1.35	1.28	1.37	1.28	25111	26038	−3.56%
ACS-14	1.26	1.21	1.23	1.21	23827	25371	−6.09%
ACS-15	1.23	1.18	1.14	1.14	23343	24606	−5.13%
ACS-16	1.14	1.11	1.09	1.09	22295	23783	−6.26%

4. Evaluation of prediction performance of proposed calculation formulas

Many earlier studies have developed calculation formulas for calculating the axial load-bearing capacity of section-enlargement columns. In this study, the typical calculation equations for section-enlargement columns have been selected to predict the load-bearing capacity of specimens listed in Table 5.

The comparison results between experiment and calculation equations were shown in Figure 15. The first three prediction calculation formulas, including the China code GB/T 50367-2013 (Ministry of Housing and Urban-rural Development of the People's Republic of China, 2014), the ACI 318-14 code (ACI, 2014) and the Eurocode 2 (European Committee for Standardization, 2005), underestimated the axial load-bearing capacity of strengthened columns. In particular, the errors of the China code and the ACI 318-14 code range from −23.41% to −32.35%. The reason was that the first two calculation formulas did not consider the confinement effect of the stirrups in the strengthened part of specimens. The calculation of Eurocode 2 adopted the compressive strength of confined concrete and the error ranges from −8.49% to −20.63%. The Liao model considered the confinement effect of concrete in strengthened part on existing columns when calculating the axial

load-bearing capacity of strengthened columns, the confinement effect of the concrete in the strengthened part of specimens is not obvious when concrete cracked. The load-bearing capacity of strengthened columns is equal to the load when concrete cracked. Thus, the Liao's (2006) model also underestimated the axial load-bearing capacity of strengthened columns. In the Zhang model (Zhang, 2016),
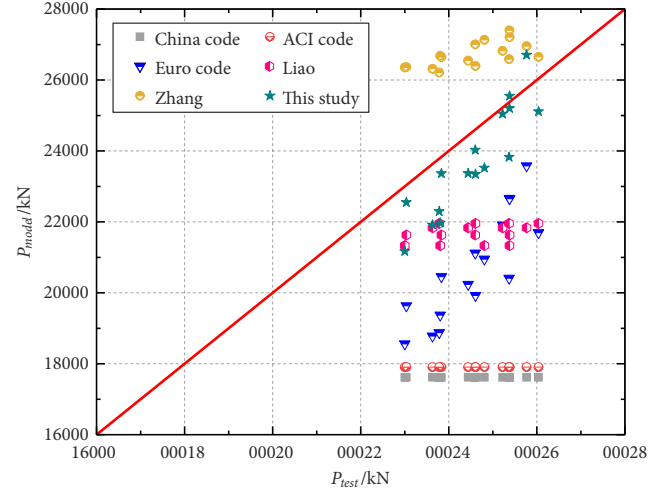

Figure 15. Comparisons results between of experiment and prediction models

Table 5. Calculation equations for predicting the axial load-bearing capacity of section-enlargement columns from earlier studies

Models	Calculation equation	Coefficients
China code GB/T 50367-2013 (Ministry of Housing and Urban-rural Development of the People's Republic of China, 2014)	$N = \varphi\left(f_{c0}A_{c0} + f'_{y0}A'_{s0} + \alpha_{cs}\left(f_{c0}A_{c0} + f'_y A'_s \right) \right)$	$\alpha_{cs} = 0.8$
ACI 318-14 code (American Concrete Institute [ACI], 2014)	$N = 0.85 f_{c0}A_{co} + 0.85 f_c A_c + f'_{y0}A'_{s0} + f'_y A'_s$	
Eurocode 2 (European Committee for Standardization, 2005)	$N = f_{cc0}A_{c0} + f_{cc}A_c + f'_{y0}A'_{s0} + f'_y A'_s$	$f_{cc} = f_c(1 + 5\dfrac{f_{le}}{f_c})$, $f_{le} < 0.05 f_c$ $f_{cc} = f_c(1.125 + 2.5\dfrac{f_{le}}{f_c})$, $f_{le} > 0.05 f_c$
Liao (2006)	$N = \varphi\left(K f_{c0}A_{c0} + f'_{y0}A'_{s0} + \alpha_c f_c A_c + \alpha_s f'_y A'_s \right)$	$K = 1 + 0.656\dfrac{b}{d}\dfrac{f_c}{f_{co}}$ $\alpha_c = 2\sqrt{1-\beta} + \beta - 1$ $\alpha_s = \dfrac{E_{s2}}{500 f'_y}\sqrt{1-\beta}$
Zhang (2016)	$N = \varphi\left((K + \gamma_{co}) f_{c0}A_{c0} + f'_{y0}A'_{s0} + \alpha_c f_c A_c + \alpha_s f'_y A'_s \right)$	$K = 1 + \dfrac{\rho_s f_{yh}}{f_c}$ $\gamma_{co} = 1 + 0.82\psi\dfrac{b}{d}\dfrac{f_c}{f_{co}}$ $\alpha_c = 2K\sqrt{1 - \dfrac{1}{K}\beta} + K\beta - K^2$ $\alpha_s = \dfrac{K E_{s2}}{500 f'_y}\sqrt{1 - \dfrac{1}{K}\beta}$

Note: N was the axial load-bearing capacity of section-enlargement columns; φ was the stability coefficient of strengthened columns; α_{cs} was the reduction coefficient of the strength of concrete and longitudinal reinforcements in strengthened part; K was the confinement coefficient of existing column; b was the thickness of strengthened part; d was the dimension of existing columns.

two coefficients were contained to evaluate the confinement effects of concrete and stirrups in strengthened part on existing columns. The prediction results from the Zhang model (Zhang, 2016) overestimated the axial load-bearing capacity of strengthened columns and the error ranges from 4.60% to 14.58%. This is because the Zhang model (Zhang, 2016) overestimated the confinement effect of strengthened part. The model developed in this study estimated the axial load-bearing capacity of strengthened columns accurately and the error ranges from –7.96% to 3.64%. Thus, the proposed model is suitable for evaluating the axial load-bearing capacity of strengthened columns.

Conclusions

In this study, an experiment consisting of sixteen large-scale concrete columns strengthened by octagonal stirrups and four spiral stirrups at the corner of specimens was carried out. The axial load-bearing capability of strengthened columns have been calculated and compared with the experimental results; the conclusions are drawn as follows:

(1) The axial compression ratio of existing column has an unfavorable effect on the axial load-carrying capacity of section-enlargement columns. The result shows that the axial load-bearing capacity of specimens decreases with the increase of axial compression ratio of existing columns when the volumetric ratio of stirrups in strengthened part keeps as a certain value.

(2) The stirrups in the strengthened part of specimens can significantly enhance the axial load-bearing capacity of section-enlargement columns with the increase of the volumetric ratio of stirrups. The octagonal stirrup and four spiral stirrups can generate high lateral confining stress and the higher volumetric ratio of stirrups resulting in the higher axial load-bearing capacity of specimens.

(3) The concrete in the cross section of section-enlargement columns can be categorized into five areas according to the confinement conditions. The evaluation model of the axial load-bearing capacity of strengthened columns developed in this study had high accuracy.

(4) The axial load-bearing capacity of section-enlargement columns has been evaluated by the existing models from the earlier studies. The existing models need to be modified by considering the confinement effects of stirrups in the strengthened part of specimens on the compressive strength of concrete.

Data availability statement

The data was from the author experiment. The experimental data was obtained by authors.

Conflicts of interest

The authors declare no conflict of interest.

References

Adilson, R. T., Joao, B. D. H., & Amir, M. (2008). Preloaded RC columns strengthened with high-strength concrete jackets under uniaxial compression. *Materials and Structures*, *41*(7), 1251–1262. https://doi.org/10.1617/s11527-007-9323-0

American Concrete Institute. (2014). *Building code requirements for structural concrete (ACI 318-14) and commentary*.

Cao, Q., Tao, J., Ma, Z. J., & Wu, Z. (2017). Axial compressive behavior of CFRP-confined expansive concrete columns. *ACI Structural Journal*, *114*(2), 475–485. https://doi.org/10.14359/51689450

Cheng, C. S. (2003). *Theoretical analysis of load capacity of reinforced concrete columns strengthened with reinforced concrete cover*. Hunan University, Hunan, China.

Ersoy, U., Suleiman, R., & Tankut, T. (1993). Behavior of jacketed columns. *ACI Structural Journal*, *90*(3), 288–293. https://doi.org/10.14359/4236

European Committee for Standardization. (2005). *Eurocode 2: Design of concrete structures: Part 1-1: general rules and rules for buildings* (EN 1992-1-1). Brussels.

Hwang, Y. H., Yang, K. H., Mun, J. H., & Kwon, S. J. (2020). Axial performance of RC columns strengthened with different jacketing methods. *Engineering Structures*, *206*, 110179. https://doi.org/10.1016/j.engstruct.2020.110179

Julio, E., & Branco, F. A. B. (2008). Reinforcing concrete jacketing-interface influence on monotonic loading response. *ACI Structural Journal*, *105*(4), 471–477. https://doi.org/10.14359/19861

Liao, W. D. (2006). *Theoretical research and application of enlarging section method in reinforcing axially loaded RC columns*. Southwest Jiaotong University, Chengdu, China.

Liu, W. (2005). *Research on mechanism of concrete-filled steel tubes subjected to local compression*. Fuzhou University, Fuzhou, China.

Luo, L. L. (1989). Calculation method of cross-section strength of concrete components strengthened by enlarged cross-section methods. *Sichuan Building Science Research*, *4*, 17–20.

Mander, J. B., & Priestley, M. J. N. (1988). Theoretical stress-strain model for confined concrete. *Journal of Structural Engineering*, *114*(8), 1804–1826. https://doi.org/10.1061/(ASCE)0733-9445(1988)114:8(1804)

Ministry of Housing and Urban-rural Development of the people's Republic of China. (2010). *Code for design of concrete structures* (GB 50010-2010). China Building Industry Press.

Ministry of Housing and Urban-rural Development of the people's Republic of China. (2012). *Standard for test method of concrete structures* (GB/T 50512-2012). China Architecture & Building Press.

Ministry of Housing and Urban-rural Development of the People's Republic of China. (2014). *Code for design of strengthening concrete structures* (GB/T 50367-2013). China Building Industry Press.

Su, S. Q., Feng, D. G., & Wang, Q. M. (1997). Calculation of load-capacity of axially compressive RC columns strengthened with enclosed reinforced concrete. *Journal of Xi'an University of Architecture and Technology*, *29*(4), 381–385.

Tang, Y. Q. (2000). *Building reconstruction and severe defect treatment*. China Building Industry Press.

Thermou, G. E., Papanikolaou, V. K., & Kappos, A. J. (2014). Flexural behavior of reinforced concrete jacketed columns under reversed cyclic loading. *Engineering Structures*, *76*, 270–282. https://doi.org/10.1016/j.engstruct.2014.07.013

Vandoros, K. G., & Dritsos, S. E. (2008). Concrete jacket construction detail effectiveness when strengthening RC columns. *Construction & Building Materials*, *22*(3), 264–276. https://doi.org/10.1016/j.conbuildmat.2006.08.019

Zhang, J. S. (2004). Development of seismic evaluation and strengthening techniques in China. *Earthquake Resistant Engineering and Retrofitting*, *5*, 33–39.

Zhang, Z. M., Xue, D. T., & Su, S. Q. (2001). Non-linear finite element analysis of RC column strengthened with enclosed reinforced concrete. *Chinese Quarterly of Mechanics*, *22*(2), 221–227.

Zhang, Z. M. (2016). *The compressive bearing capacity of normal section of RC short column reinforced by section-increased method considering secondary loading*. Fuzhou University, Fuzhou, China.